Star-planet tidal interactions in the WASP-12 system

Gracjan Maciejewski[1]

1. Institute of Astronomy, Faculty of Physics, Astronomy and Informatics, Nicolaus Copernicus University, Grudziadzka 5, 87-100 Torun, Poland

To date, the exoplanet WASP-12 b is the only hot Jupiter for which the shortening of its orbital period was detected. A mechanism that drives this orbital decay remains a puzzle. Equilibrium stellar tides alone were found to be too weak to explain the observed rate of inspiral and dynamical stellar tides or planetary obliquity tides have been considered. Compared to other stars, WASP-12 is distinguished by its extremely high efficiency of the dissipation of the tidal energy, typical rather for sub-giants than for main sequence dwarfs. Therefore, it cannot be ruled out that the system is observed at a specific moment of the stellar evolution in which the star leaves the main sequence, heading towards the red giants branch. Using the new radial velocity (RV) measurements acquired with the HARPS-N instrument at the Telescopio Nazionale Galileo, we show that the observed orbital eccentricity of WASP-12 b is non-zero at a 5-sigma level, and the longitude of pericentre of this apparently eccentric orbit is close to 270 degrees. This orbital configuration is compatible with a solution containing a circular orbit and an RV signal induced by the tidal fluid flow in the star. The amplitude of the RV tides was found to be consistent with a value calculated using the equilibrium tide approximation. This finding opens new possibilities in probing the physical properties of stellar interiors.

1 Introduction

Because of proximity to the host star, the WASP-12 b planet (Hebb et al., 2009) has become a subject of numerous studies on the planetary atmosphere and star-planet interactions. The orbital distance of just 3 stellar radii (i.e. 0.023 AU) and the irradiance from the 6300 K host star result in an equilibrium temperature of the order of 2500 K. The translucent gas of the exosphere is revealed by strong absorption lines of metals in the near-UV spectra (Fossati et al., 2010). Numerical simulations show that the exospheric gas overfills the Roche lobe and escapes via the Lagrangian L1 and L2 points, and forms a circumstellar disk (Debrecht et al., 2018).

Theoretical considerations show that planets on short-period orbits are unstable to tidal dissipation and finally spiral in toward the host star (Levrard et al., 2009; Essick & Weinberg, 2016). Tidal dissipation in the star causes the planet to lose angular momentum because energy deposited in tidal bulges is dissipated and the star is spun-up. In the equilibrium tide approximation, the tidal bulge raised in the star lags the planet when the planet's orbital period is shorter than the star's rotational period. This is the opposite of the Earth–Moon system, in which the Moon recedes from the Earth because the bulge leads the Moon. The efficiency of tidal dissipation within a star is quantified with the tidal quality factor Q_* that is the ratio of energy stored in tidal distortion and energy dissipated in one tidal cycle.

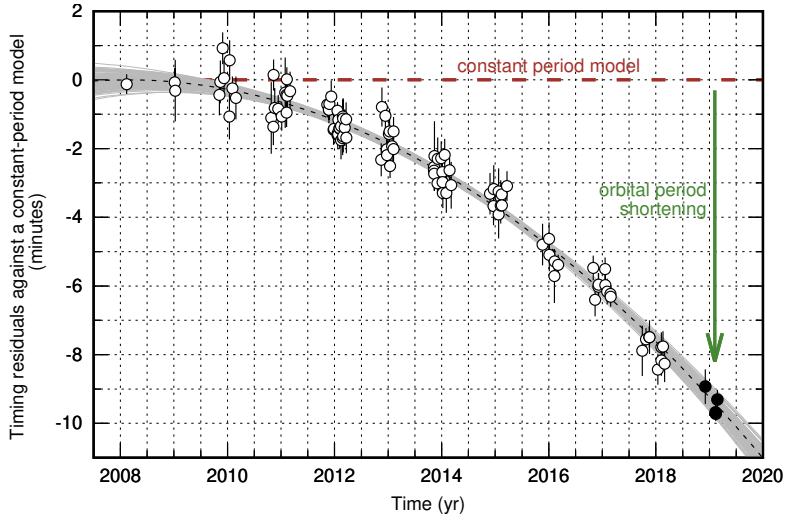

Fig. 1: Timing residuals against a constant-period model for WASP-12 b. Orbital period shortening makes transits to appear earlier following a quadratic ephemeris drawn with a black dashed line. Open circles come from a compilation of Maciejewski et al. (2018) and dots are new mid-transit times from the observing season 2018/2019, taken from Maciejewski et al. (in prep.). Grey lines illustrate ephemeris uncertainties, they are drawn for 100 sets of parameters randomly chosen from the Markov chains. The constant period model is shown with a red dashed line.

In literature, there are often used values of $Q'_* = 1.5Q_*/k_2$, where k_2 is the tidal Love number. Studies of binary stars (e.g. Meibom & Mathieu, 2005) or planetary systems with hot Jupiters (e.g. Bonomo et al., 2017) show that values of Q'_* must be of the order or greater than 10^6 for typical dwarfs. This finding suggests that dissipation is of rather low efficiency. The timescale of inspiral calculated for typical hot Jupiters is of the same of greater order as the time of stellar evolution on the main sequence. Only the most massive planets on the tightest orbits are expected to undergo the orbital shrinkage that could be detected in timescale of decades via precise transit timing (Birkby et al., 2014; Maciejewski et al., 2018).

Using the method of precise transit timing we detected shortening of the orbital period for WASP-12 b (Maciejewski et al., 2016). This departure from a linear transit ephemeris was confirmed by Patra et al. (2017) and then refined to ∼8 minutes in the course of 10 years by us (Maciejewski et al., 2018). The transit timing residuals against a linear ephemeris are shown in Fig. 1 in which new timing data from the observing season 2018/2019 are also presented. These new data points follow the quadratic ephemeris very well that strengthens the model of the in-falling planet. The value of Q'_* can be deduced from the change in the orbital period between succeeding transits $\frac{dP_{\rm orb}}{dE}$ following the formula

$$Q'_* = -\frac{27}{2}\pi \left(\frac{M_{\rm p}}{M_*}\right)\left(\frac{a}{R_*}\right)^{-5}\left(\frac{dP_{\rm orb}}{dE}\right)^{-1} P_{\rm orb}\,, \qquad (1)$$

where $M_{\rm p}$ and M_* are the planet's and star's masses, a is the semi-major axis, and R_* is the stellar radius.

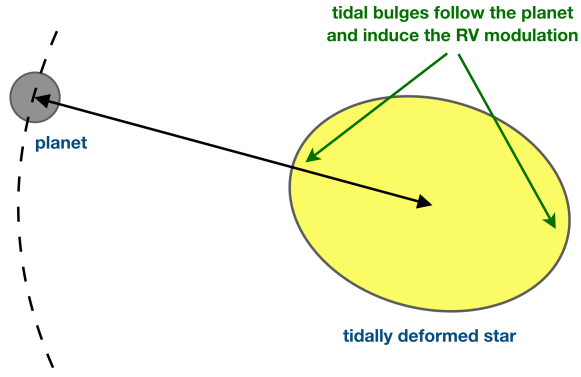

Fig. 2: Cartoon showing a tidally deformed star and a massive planet on a tight orbit as a source of the tidal force.

For WASP-12, the parameter Q'_* was found to be surprisingly low with a value of $\approx 2 \times 10^5$. The mechanism that governs this efficient dissipation of tidal energy remains a puzzle. Equilibrium stellar tides are too weak to explain the observed rate of inspiral. Dynamical stellar tides would be an efficient way to dissipate the tidal energy but they require a subgiant structure for the star (Weinberg et al., 2017). Stellar parameters, however, favour a main sequence host (Bailey & Goodman, 2019). An alternative scenario has been proposed by Millholland & Laughlin (2018) in which the high orbital decay rate is driven by obliquity tides. A spin vector of WASP-12 b would need to be trapped in a high-obliquity state maintained by a secular spin-orbit resonance with an unseen exterior perturbing planet. This additional planet would be in an orbital distance < 0.04 AU (an orbital period shorter than 2.6 d) and have a mass of $10-20\ M_\mathrm{E}$. However, such a close-by planet has not been found so far.

2 Equilibrium tide approximation

For very hot Jupiter-like exoplanets, departure of the figures of both the host star and the planet become important. The tidal force, which is raised by one body on the other, is proportional to the mass of the body rising the tide, and inversely proportional to the cube of the distance between both bodies. The orbit of the planet is expected to be circularised, and its rotation is synchronised with the orbital period. The star usually rotates slower than the planet orbits it. This picture is analogous to the Earth-Moon system except that Earth rotates faster than the Moon orbits it.

In the equilibrium tide approximation, there are some reasonable simplifications which make further consideration easier. Stellar matter is assumed to be incompressible and to follow gravitational equipotentials ignoring fluid inertia. Furthermore, the forcing frequency is set to zero, any effects induced by convective motions are neglected, and the stellar rotation is set to zero. The source of the deforming force – the planet – is assumed to be a point mass. Arras et al. (2012) show that these simplifications make predictions of the equilibrium tide approximation to be accurate to a factor of up to ≈ 2. As it is pictured in Fig. 2, equilibrium tides follow the orbital motion of the planet, and a given fluid element undergoes vertical and

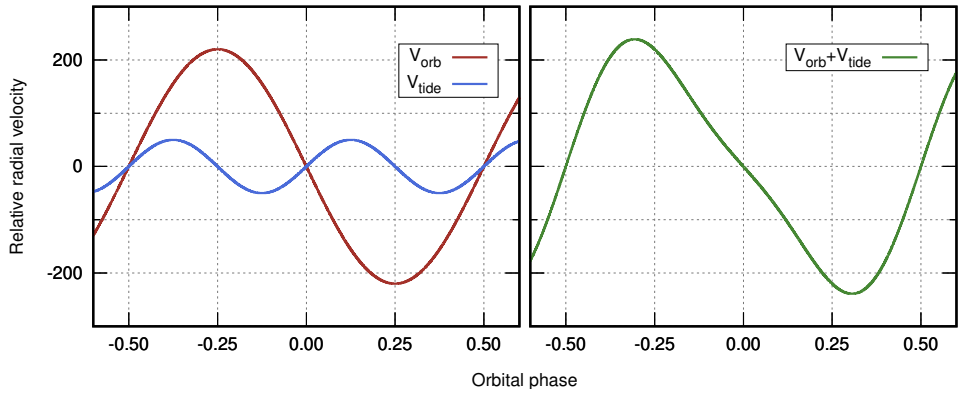

Fig. 3: Left: orbital motion component $V_{\rm orb}$ and tidal velocity component $V_{\rm tide}$ of the observed RV signal for an exemplary system with a star being tidally deformed, based on parameters of the WASP-12 system. The amplitude of $V_{\rm tide}$ is exaggerated by a factor of 10 for better visualisation. Right: observed RV signal being a sum of the orbital motion component and tidal velocity component.

horizontal motions twice per orbit.

The motion of the tidal bulges is expected to produce a radial velocity (RV) signal linked with the signal produced by the orbital motion of the planet. This tidal RV modulation has the frequency twice the orbital frequency, and is shifted in phase ϕ by π. Assuming the barycentric velocity is subtracted, the relative observed radial velocity $V_{\rm rad}(\phi)$ is a sum of the orbital motion component $V_{\rm orb}(\phi)$ and tidal velocity component $V_{\rm tide}(\phi)$ defined as

$$V_{\rm orb}(\phi) = -K_{\rm orb} \sin\left(2\pi(\phi - \phi_0)\right) \tag{2}$$

and

$$V_{\rm tide}(\phi) = K_{\rm tide} \sin\left(4\pi(\phi - \phi_0)\right) \ . \tag{3}$$

The parameters $K_{\rm orb}$ and $K_{\rm tide}$ are the amplitudes, and ϕ_0 is a relative phase offset. Both components are plotted in the left panel of Fig. 3 using the theoretical values for the WASP-12 system. Arras et al. (2012) show that $K_{\rm tide}$ could be of the order of a few meters per second for the most promising systems, so could be detected with present-day radial speedometers.

In the right panel of Fig. 3, the sum of $V_{\rm tide}$ and $V_{\rm orb}$ is plotted. As one can see, the shape of this observed curve resembles a signal produced by a planet on an eccentric orbit. So, the tidal RV component can be mimicked by an apparently non-zero orbital eccentricity $e_{\rm b}$. As demonstrated by Arras et al. (2012), this orbital configuration has a longitude of periastron equal to 270° and $K_{\rm tide} = e_{\rm b} K_{\rm orb}$.

According to the equilibrium tide approximation, the predicted value of $K_{\rm tide}$ for induced by WASP-12 b is of about $5\,{\rm m\,s^{-1}}$, and hence the value of $e_{\rm b}$ is expected to be of about 0.022. Preliminary detections of the non-zero eccentricity of WASP-12 b were reported in previous studies with low significance. In the discovery paper, Hebb et al. (2009) find $e_{\rm b} = 0.049 \pm 0.015$ and Knutson et al. (2014) report $e_{\rm b} = 0.037^{+0.014}_{-0.015}$. On the other hand, Husnoo et al. (2011) find $e_{\rm orb} = 0.018^{+0.024}_{-0.014}$ that is statistically indistinguishable from a circular model. The same conclusion was

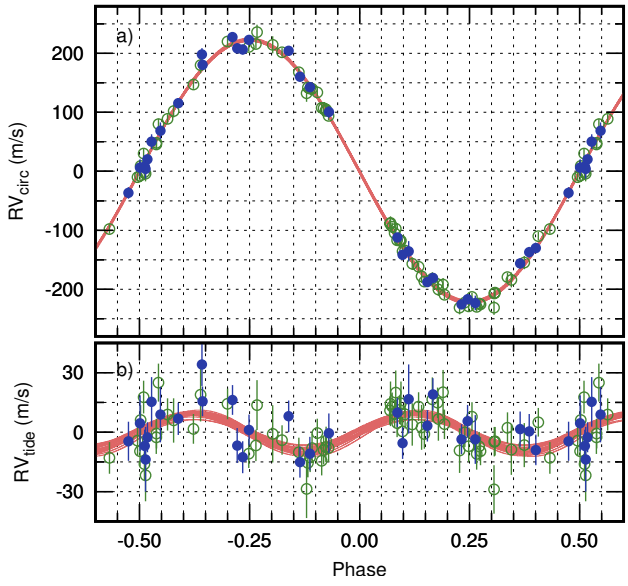

Fig. 4: Upper panel: phase-folded orbital RV component for a circular orbit of WASP-12 b (RV_{circ}). The green open symbols mark data points from the literature. The blue dots are our new measurements which were taken from Maciejewski et al. (2020). The best-fitting model and parameter uncertainties of this model are illustrated with red lines which are drawn for 50 sets of parameters, randomly chosen from the Markov chains. Stellar jitter was added in quadrature to the individual RV errors in order to obtain a reduced chi-square statistic of unity for the best-fitting model. Lower panel: tidal RV component which mimics the non-zero orbital eccentricity of WASP-12 b.

reached by Bonomo et al. (2017) who were only able to constrain e_b to 0.02 with a $1\,\sigma$ level.

3 Radial velocity tides

Circularisation timescale for WASP-12 b's orbital configuration is about 0.4 Myr. This is much shorter than the system age which is estimated to be 4 orders of magnitude longer. Thus, the orbit of WASP-12 b is expected to be circular unless there is an efficient mechanism which excites and sustains the non-zero eccentricity. As discussed in Bailey & Goodman (2019), no such mechanism has been identified so far.

Our analysis of the RV measurements reveals that the orbit of WASP-12 b shows the apparent departure from circularity that can be naturally explained by the velocity signature of tidal deformations in the host star. We used the high precision RV data from Knutson et al. (2014), Bonomo et al. (2017), and new velocities acquired by us with the High Accuracy Radial velocity Planet Searcher in the northern hemisphere (HARPS-N) coupled with the 3.58 m Telescopio Nazionale Galileo (Maciejewski et al., 2020). The observations acquired during in-transit phase were removed to avoid disturbances caused by the Rossiter-McLaughlin effect. In addition, a $5\,\sigma$ outliers were iteratively removed in fitting procedure. The best-fitting

Keplerian solution was found with the Levenberg-Marquardt method, and parameters' uncertainties were estimated with the bootstrap algorithm using 10^5 resampled datasets.

We find that $e_{\rm b} = 0.0331 \pm 0.0056$ and $\omega = 270.5^\circ \pm 0.8^\circ$. This is a $5.9\,\sigma$ detection of the non-circular orbit. Its orientation is consistent within a 1σ level with the specific way that is degenerated with the tidal RV signal. Fig. 4 presents the orbital and tidal components of the observed RV variations. We derived $K_{\rm tide} = 7.4 \pm 0.5$ m s^{-1}.

4 Conclusions

We have found that the orbit of WASP-12 b appears to be apparently eccentric with the periastron longitude close to 270°. As the actual eccentricity must be zero, this specific configuration is naturally interpreted as the RV manifestation of the tidal deformation of the host star that follows the orbital motion of the planet. The RV amplitude of the tides $K_{\rm tide}$ of ~ 7.4 m s^{-1} corresponds to the height of tides up to ~ 150 km in the star. As the predictions of the equilibrium tide approximation are accurate to a factor of ~ 2 (Arras et al., 2012), the reported here value of $K_{\rm tide}$ can be considered as being consistent with the theory. We note, however, that development of more advanced models would benefit in our better understanding of star-planet tidal interactions.

Acknowledgements. The author acknowledge the financial support from the National Science Centre, Poland through grant No. 2016/23/B/ST9/00579.

References

Arras, P., Burkart, J., Quataert, E., Weinberg, N. N., *MNRAS* **422**, 1761 (2012)

Bailey, A., Goodman, J., *MNRAS* **482**, 2, 1872 (2019)

Birkby, J. L., et al., *MNRAS* **440**, 1470 (2014)

Bonomo, A. S., et al., *A&A* **602**, A107 (2017)

Debrecht, A., et al., *MNRAS* **478**, 2592 (2018)

Essick, R., Weinberg, N. N., *ApJ* **816**, 18 (2016)

Fossati, L., et al., *ApJ* **714**, L222 (2010)

Hebb, L., et al., *ApJ* **693**, 1920 (2009)

Husnoo, N., et al., *MNRAS* **413**, 2500 (2011)

Knutson, H. A., et al., *ApJ* **785**, 126 (2014)

Levrard, B., Winisdoerffer, C., Chabrier, G., *ApJ* **692**, L9 (2009)

Maciejewski, G., et al., *A&A* **588**, L6 (2016)

Maciejewski, G., et al., *Acta Astron.* **68**, 4, 371 (2018)

Maciejewski, G., et al., *ApJ* **889**, 1, 54 (2020)

Meibom, S., Mathieu, R. D., *ApJ* **620**, 970 (2005)

Millholland, S., Laughlin, G., *ApJ* **869**, 1, L15 (2018)

Patra, K. C., et al., *AJ* **154**, 4 (2017)

Weinberg, N. N., Sun, M., Arras, P., Essick, R., *ApJ* **849**, 1, L11 (2017)